

Modulation of Majorana induced current cross-correlations by quantum dots

Björn Zocher^{1,2} and Bernd Rosenow¹

¹*Institut für Theoretische Physik, Universität Leipzig, D-04103 Leipzig, Germany*

²*Max Planck Institut für Mathematik in den Naturwissenschaften, D-04103 Leipzig, Germany*

(Dated: August 21, 2012)

We study charge transport through a topological superconductor with a pair of Majorana end states, coupled to leads via quantum dots with resonant levels. The non-locality of the Majorana bound states opens the possibility of crossed Andreev reflection with nonlocal shot noise, due to the injection of an electron into one end of the superconductor followed by the emission of a hole at the other end. In the space of energies of the two resonant quantum dot levels, we find a four peaked clover-like pattern for the strength of noise due to crossed Andreev reflection, distinct from the single ellipsoidal peak found in the absence of Majorana bound states.

PACS numbers: 03.75.Lm, 74.45.+c, 74.78.Na, 73.21.-b

Majorana bound states (MBSs) are zero-energy fermionic states which are their own anti-particles. Since quasi-particles (QPs) in superconductors (SCs) are always superpositions of electron and hole components, the Majorana criterion can be realized in a peculiar way: a zero energy QP in an SC has equal contributions from electrons and holes, and hence an exchange of particle and hole components leaves the QP invariant. There is currently much interest in the physics of MBSs [1–8], since one pair of MBSs nonlocally encodes a qubit, which is the building block for fault-tolerant topological quantum computing architectures.[9, 10]

There is a variety of candidate systems for realizing Majorana fermions. Early proposals considered time-reversal symmetry broken p -wave SCs with the candidate Sr_2RuO_4 . [11] Recently, the superconducting proximity effect has been suggested as a way to effectively induce p -wave pairing in topological insulators [12] and semiconductors with strong Rashba spin-orbit coupling.[13–16] Recent experiments reported evidence of Majorana bound states (MBSs) in semiconductor-superconductor heterostructures.[1–5] A possible probe for the nonlocal nature of MBSs is crossed Andreev reflection (CAR), the conversion of an incoming electron into an outgoing hole in a different lead, [17–22] in contrast to local Andreev reflection (LAR), where electron and hole reside in the same lead. It has been shown theoretically that at sufficiently low voltages and small level width, LAR by a pair of MBSs is fully suppressed in favor of CAR.[23–27] For voltages larger than the MBS energy splitting ϵ_M however, local scattering processes dominate and suppress the crossed noise.

Motivated by recent measurements of nonlocal transport in s -wave SCs coupled to quantum dots (QDs) [28, 29], in this letter we study non-local transport through a coupled dot-MBS system as sketched in Fig. 1. In this setup, the QDs are used to suppress LAR due to Coulomb blockade. We consider a single-channel wire with one MBS located at each end. Each MBS is coupled to the adjacent lead via a quantum dot in the

Coulomb blockade regime, modeled by a level of width Γ . Due to the finite wire length, the MBSs are tunnel coupled to each other and have an energy splitting $\epsilon_M \sim \Delta \exp(-L/\xi_{SM})$, where ξ_{SM} is the coherence length in the semiconductor. This tunnel coupling makes nonlocal CAR possible and gives rise to current cross-correlations $\propto (e^2/h)\epsilon_M^2/\Gamma$. In the regime $\Gamma \ll \epsilon_M$, transport occurs via discrete resonances, and CAR is suppressed if one dot level is resonant with the SC. This is due to the formation of a zero-energy Majorana mode residing in the resonant dot, [30] which cannot contribute to current cross-correlations since it has no energy splitting. The second regime $\Gamma \gg \epsilon_M$ can be more easily realized experimentally. For large voltages $eV \gg \epsilon_M$, the crossed current correlator now has a four-leaf clover feature as a function of the dot levels ϵ_L and ϵ_R . The extension of this structure is determined by Γ , with a suppression of the noise when at least one dot is resonant with the SC. In striking contrast, the crossed noise for two dots with a non-resonant proximity coupling shows a single-peak structure with dominant weight along $\epsilon_L = -\epsilon_R$. [21, 22, 29] These findings are in excellent agreement with results for a microscopic model of a spinless p -wave superconductor. [31]

Model system.— We consider the Hamiltonians

$$H_D = \sum_{i=L,R} \left(\epsilon_i d_i^\dagger d_i + g_i d_i^\dagger \psi_i + g_i^* \psi_i^\dagger d_i \right), \quad (1a)$$

$$H_M = \epsilon_M i \gamma_L \gamma_R + \sum_{i=L,R} (t_i d_i^\dagger \gamma_i + t_i^* \gamma_i d_i), \quad (1b)$$

$$H_S = \Delta (d_L^\dagger d_R^\dagger + d_R d_L). \quad (1c)$$

Here, H_D describes two QDs coupled to leads, where d_i annihilates an electron with energy ϵ_i on dot i , ψ_i annihilates a lead electron, and g_i is the lead-dot coupling strength. The lead electrons are characterized by their density of states ρ_i , which is assumed to be energy independent, and have a chemical potential eV . We consider the regime where the QD single particle level spacing $\delta\epsilon > eV > k_B T$, assume that the spin degeneracy is

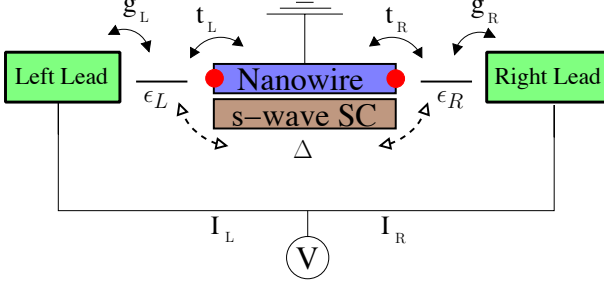


FIG. 1. (color online) Schematic setup for a system with a pair of Majorana bound states (red dots) coupled to quantum dots which themselves are coupled to lead electrodes. The leads are biased with the positive chemical potential eV . Crossed Andreev reflection can be detected by correlating the currents I_L and I_R that flow into the SC nanowire via MBSs. The nearby s -wave SC also induces a proximity pairing Δ between the dots.

lifted by an external magnetic field, and that the QD ground state has an even number of electrons. Then, Kondo physics is absent and in the Coulomb blockade regime inclusion of only a single dot level in H_D is justified. H_M describes two MBSs with an energy splitting ϵ_M coupled to the dots. The MBSs are described by hermitian operators $\gamma_i = \gamma_i^\dagger$, which have anti-commutators $\{\gamma_i, \gamma_j\} = 2\delta_{i,j}$, and are coupled to QD i with amplitude t_i . The chemical potential of the superconducting wire hosting the MBS is zero. H_S describes an additional proximity induced pairing between the dots with an amplitude $\Delta \sim \gamma_S \sin(k_F L) \exp(-L/\xi_{SC})/(k_F L)$ [21], where γ_S is the normal-state QD level broadening due to the coupling between SC and QD, k_F the Fermi momentum, L the wire length, and ξ_{SC} the coherence length of the SC. We have in mind that this term may mainly be due to a coupling between the dots and the s -wave superconductor in a hybrid structure.

We diagonalize the Hamiltonian for MBSs and QDs without lead coupling by solving the corresponding BdG equation $h\Psi = \epsilon(\mathbb{I}_D + \frac{1}{2}\mathbb{I}_M)\Psi$ with

$$h = \begin{pmatrix} 0 & i\epsilon_M & t_L & 0 & -t_L^* & 0 \\ -i\epsilon_M & 0 & 0 & t_R & 0 & -t_R^* \\ t_L^* & 0 & \epsilon_L & 0 & 0 & \Delta \\ 0 & t_R^* & 0 & \epsilon_R & -\Delta & 0 \\ -t_L & 0 & 0 & -\Delta & -\epsilon_L & 0 \\ 0 & -t_R & \Delta & 0 & 0 & -\epsilon_R \end{pmatrix} \quad (2)$$

in the basis $\{\gamma_L, \gamma_R, d_L^\dagger, d_R^\dagger, d_L, d_R\}$. Here, \mathbb{I}_D (\mathbb{I}_M) denote the identity matrix in the dot (Majorana) space. In the case $\Delta = 0$, the quasiparticle energy spectrum has levels at $2\epsilon_M$, ϵ_R , and ϵ_L , with avoided crossings where these levels intersect each other. If one of the QD energies is zero, the spectrum has a zero-energy MBS.

To compute the zero-frequency noise through the above normal-SC-normal (NSN) system, we use a scattering matrix approach which also allows for Andreev

reflection processes.[32] This yields the current and the noise correlators

$$I_i = \frac{e}{h} \int d\epsilon \sum_{\alpha} \text{sign}(\alpha) \sum_{k;\gamma} A_{k,k;\gamma,\gamma}^{(i\alpha)} n_{k,\gamma}, \quad (3)$$

$$S_{ij} = \frac{2e^2}{h} \int d\epsilon \sum_{\alpha,\beta} \text{sign}(\alpha\beta) \sum_{k,l;\gamma,\delta} A_{k,l;\gamma,\delta}^{(i\alpha)} A_{l,k;\delta,\gamma}^{(j\beta)} n_{k,\gamma} (1 - n_{l,\delta}), \quad (4)$$

where Greek indices denote electron (e) and hole (h) channels, $\text{sign}(e) = +1$ and $\text{sign}(h) = -1$, Latin indices denote the left (L) and right (R) lead, and

$$A_{k,l;\beta,\gamma}^{(i\alpha)} = \delta_{ik} \delta_{il} \delta_{\alpha\beta} \delta_{\alpha\gamma} - s_{i,k}^{\alpha\beta*} s_{i,l}^{\alpha\gamma}. \quad (5)$$

The reservoir distribution functions $n_{k,\gamma}$ are Fermi function with different chemical potentials for the electron and hole bands $n_{k,\gamma} = 1/(1 + \exp(\beta(\epsilon - \text{sign}(\gamma)eV_k)))$. For the setup Fig. 1, $V_L = V_R \equiv V$. The coefficients $s_{i,j}^{\alpha,\beta}$ are the elements of the S -matrix

$$S(\epsilon) = 1 - 2\pi i W^\dagger \left[\epsilon \mathbb{I}_D + \frac{\epsilon}{2} \mathbb{I}_M - h + i\pi W W^\dagger \right]^{-1} W, \quad (6)$$

where W describes the coupling between the states of the system without leads and the scattering states in the leads, and $[\epsilon(\mathbb{I}_D + \frac{1}{2}\mathbb{I}_M) - h + i\pi W W^\dagger]^{-1}$ is the retarded electron Green function for the closed system with self-energy $i\pi W W^\dagger$. The coupling matrix W in the lead basis $\{\psi_L^\dagger, \psi_R^\dagger, \psi_L, \psi_R\}$ is given by

$$W_{i_1\alpha_{i_1}, i_d\alpha_{i_d}} = \text{sign}(\alpha_{i_d}) g_{i_1} \sqrt{\rho_{i_1}} \delta_{i_1, i_d} \delta_{\alpha_{i_1}, \alpha_{i_d}}, \quad (7)$$

where α_{i_d} (α_{i_1}) denotes the particle species of QD i_d (lead i_1). The coupling strengths g_i give rise to the level broadening $\Gamma_i = 2\pi\rho_i|g_i|^2$ in the dots. In the following, we consider the case $\Gamma_L = \Gamma_R \equiv \Gamma$, $t_L = t_R \equiv t$, and take the limit of zero temperature.

Weak dot-lead coupling.— We begin our analysis in the regime $\Delta = 0$ and $\Gamma < t < \epsilon_M$. In Fig. 2, both differential conductance and crossed current correlator S_{LR} are displayed as a function of bias voltage for several characteristic points in the ϵ_L - ϵ_R -plane. The differential conductance is peaked at the eigenenergies of Eq. (2). The peak width is determined by the broadening Γ . If one of the dot levels resides at the chemical potential of the SC, e.g. $\epsilon_L = 0$, we always find one zero-energy state described by the Majorana operators

$$\gamma_1 = d_L^\dagger + d_L, \quad (8)$$

$$\gamma_2 = \frac{d_R^\dagger + d_R + \frac{\epsilon_R}{t} \left[\gamma_R + i\frac{\epsilon_M}{2t} (d_L^\dagger - d_L) \right]}{\sqrt{1 + \frac{\epsilon_R^2}{t^2} \left(1 + \frac{\epsilon_M^2}{4t^2} \right)}}. \quad (9)$$

Here, γ_1 is localized on the resonant dot, while γ_2 is partially delocalized, and the weight of γ_2 on the resonant

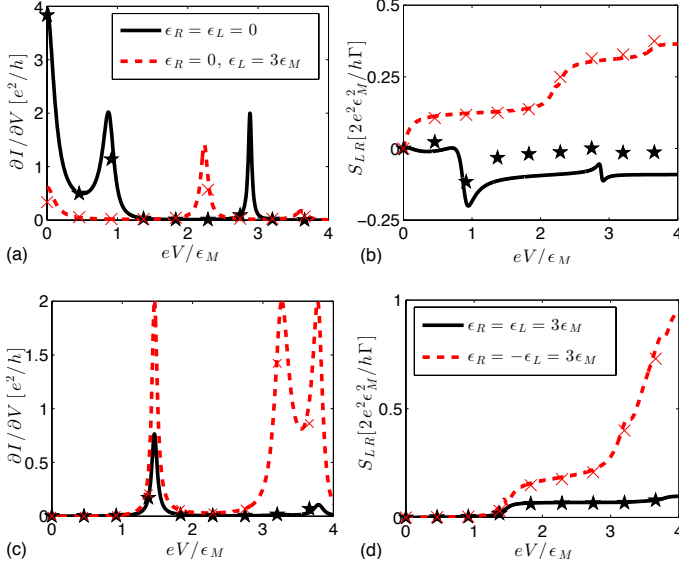


FIG. 2. (color online) Current cross-correlator S_{LR} in the weak dot-lead coupling regime with $\Gamma = \epsilon_M/4$, $t = 0.8\epsilon_M$, and $\Delta = 0$. The lines for panel (b) are defined in (a), those for panel (c) in (d). The markers denote the results for the spinless SC model with $\epsilon_M = 0.01$ meV and $\Gamma = 0.002$ meV.

dot is determined by the energy ϵ_R of the non-resonant level. At the special point $\epsilon_L = \epsilon_R = 0$, we find $\gamma_2 = d_R^\dagger + d_R$. In either case, the differential conductance has a zero bias peak with height $4(e^2/h)[t^4/(t^4 + \epsilon_M^2\epsilon_R^2/4)]$. Since the existence of a zero-energy MBS favors LAR over CAR,[25] we find that these resonances are dominated by LAR and yield only a small contribution to the crossed noise despite their large conductance.

In contrast, we do not find a zero-bias conductance peak if both dots are non-resonant. In this regime, there is a striking difference between symmetric ($\epsilon_L = \epsilon_R$) and anti-symmetric ($\epsilon_L = -\epsilon_R$) positions of the dot levels. In both cases, we find contributions to the conductance and S_{LR} due to the hybridization between the dots and the MBS. However, in the anti-symmetric case both the conductance and S_{LR} are much larger than in the symmetric case, and additional resonances at the QD energies contribute to crossed noise. This is due to the fact that Cooper pairs have zero energy, which leads to a suppression of transmission through two resonant levels which have both the same energy in the symmetric case, but allows passage through QDs with opposite level energies in the anti-symmetric case.

These findings agree very well with results for the microscopic model of a spinless p-wave SC defined in Eq. (10), see Fig. 2. The only small deviation in S_{LR} can be seen if both dots are resonant, where the effective model has a small negative S_{LR} for large bias voltage, while it approaches zero for the microscopic model. This deviation has its origin in the presence of an additional transport channel due to a proximity coupling Δ in the

microscopic model, which in principle could be described by the Hamiltonian H_S in Eq. (1c), but which is not included in the effective model $H = H_M + H_D$ considered here.

Strong dot-lead coupling.—We consider the case $t < E_M \ll \Gamma$ and begin with the situation $\Delta = 0$. In Fig. 3(a), the correlator S_{LR} for $E_M \ll eV = \Gamma/2$ in the ϵ_L - ϵ_R -plane is shown. It is characterized by a four-leaf clover feature with a suppression of crossed noise along lines with either $\epsilon_L = 0$ or $\epsilon_R = 0$, and peaks at $|\epsilon_L| = |\epsilon_R| \approx \Gamma/2$. While the peak height scales with ϵ_M^2/Γ , the width of these peaks is larger than the Majorana energy splitting due to the large value of Γ . As before, the suppression of the noise along $\epsilon_L = 0$ and $\epsilon_R = 0$ is mediated by the formation of zero-energy Majorana modes by virtue of the dot-MBS coupling, which favor the LAR transport channel.

The emergence of an approximate symmetry between symmetric and anti-symmetric positions of the dot levels (absent in the case $\Gamma < t$) can be understood as follows. For large Γ , the dots are strongly coupled to the leads and effectively become part of them. Hence, there are no separate resonances at the positions of the QD levels anymore, and only a single resonance due to the MBS in the wire survives. Since $t \ll \Gamma$, the broadening of this resonance is much smaller than Γ . As the QD levels can neither resolve this small broadening of the resonance, nor resolve the location of the resonance, the distinction between symmetric and anti-symmetric QD levels becomes blurred, and the approximate symmetry arises. The Majorana zero energy state residing on one of the dots for $\epsilon_L = 0$ or $\epsilon_R = 0$ however does not change its character due to the presence of a large broadening Γ , and the noise stays low in this case, giving rise to the clover-like pattern in Fig. 3(a).

In Fig. 3(b), we complement these findings with results for the microscopic model Eq. (10), for which a similar four-leaf clover structure emerges. However, sim-

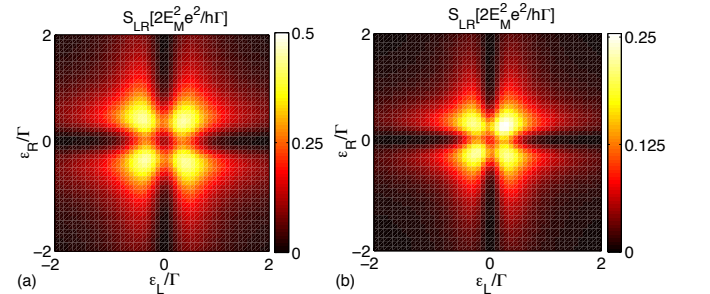


FIG. 3. (color online) Current cross-correlator S_{LR} for strong dot-lead coupling. (a) Effective model with $eV = \Gamma/2$, $t = \Gamma/20$, $\epsilon_M = \Gamma/10$, and $\Delta = 0$. (b) Spinless SC with $\epsilon_M = 0.01$ meV and $\Gamma = 0.06$ meV. For both (a) and (b), the pattern changes little for larger eV .

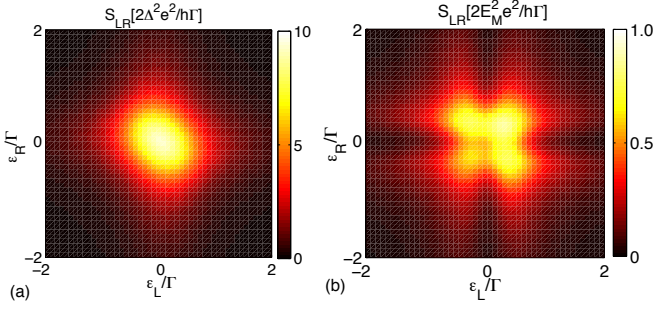


FIG. 4. (color online) Current cross-correlator S_{LR} for $eV = \Gamma/2$. The dots are coupled (a) via the SC proximity effect with $\Delta = \Gamma/10$ and (b) via SC proximity effect and with coupling to a pair of MBS with $t = \Gamma/20$, $\Delta = \Gamma/20$, and $\epsilon_M = \Gamma/10$.

ilarly to the weak dot-lead coupling regime, there are small deviations with respect to the effective model near $\epsilon_L = \epsilon_R = 0$, mediated by the SC proximity effect.

To gain insight into the effect of an additional proximity term H_S , we first discuss the situation without MBS, $H = H_D + H_S$. In Fig. 4(a), the crossed current correlator for the SC proximity case is shown. Here, S_{LR} has a single peak of height $\propto \Delta^2/\Gamma$ near $\epsilon_L = \epsilon_R = 0$, with width Γ along the direction $\epsilon_L = \epsilon_R$, and width eV along the direction $\epsilon_L = -\epsilon_R$. In contrast to the MBS case, there is no additional structure in this peak.

In figure 4(b), we consider the combined Hamiltonian $H = H_M + H_D + H_S$. We find a four-leaf clover feature similar to that in the Majorana only case, with the center of this feature now having a peak due to the proximity term in H_S . From this, we conclude that the contributions from the proximity effect and the MBS mediated CAR approximately add up. The relative peak heights in the crossed current correlator reflect the ratio of Δ^2 and ϵ_M^2 .

Microscopic model.— We complement our calculations by the analysis of a microscopic model for a spinless p -wave superconductor with Hamiltonian,[31]

$$H_K = - \sum_{j=1}^{N-1} \left(t_K c_{j+1}^\dagger c_j + \Delta_K c_j c_{j+1} + h.c. \right) - \mu_K \sum_j c_j^\dagger c_j, \quad (10)$$

where the c_j annihilate a spinless fermion on site j with nearest neighbor hopping t_K and nearest neighbor pairing amplitude Δ_K . This model describes the low-energy physics of a nanowire in the topologically non-trivial phase. In the numerical analysis, we use the parameters $L = 1000$ nm for the wire length, $N = 200$ sites, $t_K = 20$ meV, $\Delta_K = 0.8$ meV, and $\mu_K = 39.4$ meV, similar to the parameters used in [33]. These parameter values yield the SC gap $\Delta_{SC} = 0.3$ meV and the Majorana energy splitting $\epsilon_M = 0.01$ meV. For the coupling of the operators c_1 and c_N to the dots, we use

$t_{D,K} = 0.025$ meV. The results for this model agree very well with those for the effective model Eq. (1), see Figs. 2 and 3.

Conclusion.— The nonlocality of a pair of Majorana bound states can be probed by crossed Andreev reflection, whose observation is facilitated when suppressing local Andreev reflection with the help of two resonant QDs. In the case of a weak coupling between QDs and leads, we find a set of discrete transmission resonances. When at least one of the QD levels is tuned to the chemical potential of the superconductor, a zero energy Majorana state forms in the respective QD, which contributes only weakly to crossed Andreev reflection. This feature survives in the limit of strong dot-lead coupling, giving rise to a clover-like modulation of crossed shot noise as a function of QD energies, which is different from the single peak found without Majorana states.

While finalizing this manuscript, we became aware of the preprint [34], where noise in a setup similar to ours is studied using a rate equation approach.

We acknowledge helpful discussions with A. Das, M. Heiblum, and M. Horsdal, as well as financial support from BMBF.

-
- [1] V. Mourik, K. Zuo, S. M. Frolov, S. R. Plissard, E. P. A. M. Bakkers, and L. P. Kouwenhoven, *Science*, **336** 1003, 2012.
 - [2] J. R. Williams, A. J. Bestwick, P. Gallagher, Seung Sae Hong, Y. Cui, Andrew S. Bleich, J. G. Analytis, I. R. Fisher, and D. Goldhaber-Gordon. arXiv:1202.2323, 2012.
 - [3] L. P. Rokhinson, X. Liu, and J. K. Furdyna. arXiv:1204.4212, 2012.
 - [4] M. T. Deng, C. L. Yu, G. Y. Huang, M. Larsson, P. Caroff, and H. Q. Xu. arXiv:1204.4130, 2012.
 - [5] A. Das, Y. Ronen, Y. Most, Y. Oreg, M. Heiblum, and H. Shtrikman, arXiv:1205.7073
 - [6] C. W. J. Beenakker, arXiv: 1112.1950.
 - [7] J. Alicea, arXiv: 1202.1293.
 - [8] M. Leijnse and K. Flensberg, arXiv:1206.1736.
 - [9] A.Y. Kitaev, *Annals of Physics* **303**, 2 (2003).
 - [10] J. Alicea, Y. Oreg, F. von Oppen and M.P.A. Fisher, *Nature Physics* **7**, 412 (2011).
 - [11] S. Das Sarma, C. Nayak, and S. Tewari, *Phys. Rev. B* **73**, 220502(R) (2006).
 - [12] L. Fu and C.L. Kane, *Phys. Rev. Lett.* **100**, 096407 (2008).
 - [13] J. D. Sau, R. M. Lutchyn, S. Tewari, and S. Das Sarma, *Phys. Rev. Lett.* **104**, 040502 (2010).
 - [14] J. Alicea, *Phys. Rev. B* **81**, 125318 (2010).
 - [15] R. M. Lutchyn, J. D. Sau, and S. Das Sarma, *Phys. Rev. Lett.* **105**, 077001 (2010).
 - [16] Y. Oreg, G. Refael, and F. von Oppen, *Phys. Rev. Lett.* **105**, 177002 (2010).
 - [17] J. M. Byers and M. E. Flatté, *Phys. Rev. Lett.* **74**, 306 (1995).
 - [18] S. G. den Hartog, C. M. A. Kapteyn, B. J. van Wees, T.

- M. Klapwijk, and G. Borghs, Phys. Rev. Lett. **77**, 4954 (1996).
- [19] Th. Martin, Phys. Lett. A **220**, 137 (1996).
- [20] G. Lesovik, T. Martin, and G. Blatter, Eur. Phys. J. B **24**, 287 (2001).
- [21] P. Recher, E. V. Sukhorukov, and D. Loss, Phys. Rev. B **63**, 165314 (2001).
- [22] J. Rech, D. Chevallier, T. Jonckheere, and T. Martin, Phys. Rev. B **85**, 035419 (2012).
- [23] K. T. Law, P. A. Lee, and T. K. Ng, Phys. Rev. Lett. **103** 237001 (2009).
- [24] C. J. Bolech and E. Demler, Phys. Rev. Lett. **98**, 237002 (2007).
- [25] J. Nilsson, A. R. Akhmerov, C. W. J. Beenakker, Phys. Rev. Lett. **101**, 120403 (2008).
- [26] B. H. Wu and J. C. Cao, Phys. Rev. B **85**, 085415 (2012).
- [27] A. Golub and B. Horovitz, Phys. Rev. B **83**, 153415 (2011).
- [28] L. Hofstetter, S. Csonka, J. Nygård, and C. Schönenberger, Nature **461**, 960 (2009).
- [29] A. Das, Y. Ronen, M. Heiblum, D. Mahalu, A. V. Kretinin, and H. Shtrikman, arXiv:1205.2455.
- [30] M. Leijnse and K. Flensberg, arXiv:1207.4299.
- [31] A. Y. Kitaev, Physics-Uspekhi **44**, 131 (2001).
- [32] M. P. Anantram and S. Datta, Phys. Rev. B **53**, 16390 (1996).
- [33] B. Zocher, M. Horsdal, and B. Rosenow, arXiv:1111.6527.
- [34] H.-F. Lü, H.-Z. Lu, S.-Q. Shen, arXiv:1208.3070.